Experimental Conversion of a Defensin into a Neurotoxin: Implications for Origin of Toxic Function

Shunyi Zhu,*[,1] Steve Peigneur,[†,2] Bin Gao,[†,1] Yoshitaka Umetsu,[†,3] Shinya Ohki,*[,3] and Jan Tytgat*[,2]

[1]Group of Animal Innate Immunity, State Key Laboratory of Integrated Management of Pest Insects & Rodents, Institute of Zoology, Chinese Academy of Sciences, Chaoyang District, Beijing, China

[2]Toxicology and Pharmacology, University of Leuven, Leuven, Belgium

[3]Center for Nano Materials and Technology (CNMT), Japan Advanced Institute of Science and Technology (JAIST), Nomi, Ishikawa, Japan

[†]These authors contributed equally to this work.

***Corresponding author:** E-mail: Zhusy@ioz.ac.cn; shinya-o@jaist.ac.jp; Jan.tytgat@pharm.kuleuven.be.

Associate editor: Nicolas Vidal

Abstract

Scorpion K^+ channel toxins and insect defensins share a conserved three-dimensional structure and related biological activities (defense against competitors or invasive microbes by disrupting their membrane functions), which provides an ideal system to study how functional evolution occurs in a conserved structural scaffold. Using an experimental approach, we show that the deletion of a small loop of a parasitoid venom defensin possessing the "scorpion toxin signature" (STS) can remove steric hindrance of peptide-channel interactions and result in a neurotoxin selectively inhibiting K^+ channels with high affinities. This insect defensin-derived toxin adopts a hallmark scorpion toxin fold with a common cysteine-stabilized α-helical and β-sheet motif, as determined by nuclear magnetic resonance analysis. Mutations of two key residues located in STS completely diminish or significantly decrease the affinity of the toxin on the channels, demonstrating that this toxin binds to K^+ channels in the same manner as scorpion toxins. Taken together, these results provide new structural and functional evidence supporting the predictability of toxin evolution. The experimental strategy is the first employed to establish an evolutionary relationship of two distantly related protein families.

Key words: **experimental evolution, functional diversification, potassium channel, parasitic wasp, scorpion toxin, venom.**

Introduction

Understanding the molecular events of functional innovation of proteins is of general significance in evolutionary biology and of direct relevance to rational design of therapeutic drugs (Park et al. 2006). As a group of distinct organisms, venomous animals, such as sea anemones, cone snails, scorpions, spiders, shrews, lizards, and snakes, have evolved a variety of gene-encoded toxic proteins (toxins) to capture their prey and defend themselves (Brodie 2009; Fry et al. 2009). Although evolutionary emergence of toxins from proteins of physiological functions has convergently occurred in many phylogenetically diverse animal lineages and clearly it represents a successful strategy for ecological adaptation of animals, it is not clear where and how these toxins originated. On the basis of phylogenetic evidence, it has been proposed that snake toxins could have originated from their related body proteins (Fry 2005). This proposal is consistent with the observation that some ion channel-targeted neurotoxins and antimicrobial defensins share a conserved three-dimensional (3D) fold (e.g., cysteine-stabilized α-helical and β-sheet [CSαβ] fold; inhibitor cystine knot [ICK] fold; and β-defensin fold) (Zhu et al. 2003, 2005; Torres and Kuchel 2004). A combination of evolutionary, structural, and mechanistic data has also illustrated the structure–function relationships between antimicrobial peptides (AMPs) and cysteine-stabilized toxins due to common ancestry (Yount et al. 2009). It appears to be clear that throughout evolution, numerous proteins have been recruited into venoms of various animals (Fry et al. 2009). All these proteins and their evolutionarily related toxins provide an ideal system in which to study how functional innovation occurred in these tightly folded molecules.

Based on structural similarity, it was proposed that scorpion toxins and antimicrobial invertebrate defensins could have a common ancestor (Bontems et al. 1991; Kobayashi et al. 1991), a hypothesis which was subsequently strengthened based on multidimensional evidence by Froy and Gurevitz (1998), and further elaborated by Zhu et al. (2005). To address how a nontoxic protein developed into a toxin, we are studying the evolution of scorpion venom-derived toxins affecting voltage-gated K^+ channels (K_v) (abbreviated as α-KTxs). These toxins are part of the scorpion venom arsenal and most of them impair functions of K_v channels in animal neuronal membranes by binding to the channel pores to block the passage of K^+ ions (Possani et al. 1999; Tytgat et al. 1999; Garcia et al. 2001; Rodriguez de la Vega and Possani 2004). They constitute a group of evolutionarily related polypeptides, all adopting a CSαβ fold and usually containing 23–42 amino acids with three or four disulfide bridges. Most α-KTxs bind to K_v channels in a similar manner, in which a conserved lysine side chain protruding from the interacting surface of the toxins inserts in the K^+ channel pore to make intimate contact with the selectivity filter

Article

Fast Track

(Garcia et al. 2001; Lange et al. 2006). Insect defensins are an essential component of the innate immune system of invertebrates, and they often destroy the cytoplasmic membrane of Gram-positive bacteria through a channel-forming mechanism of membrane permeabilization (Dimarcq et al. 1998; Takeuchi et al. 2004). Apart from Protostomes (e.g., arthropoda and mollusca), some species belonging to Deuterostomes (e.g., amphioxus) and even fungi also contain classical insect-type defensins (CITDs) (Yu et al. 2008; Zhu 2008; Xu and Faisal 2010) (supplementary fig. S1, Supplementary Material online), which supports an ancestral position of the defensins relative to scorpion toxins (Rodríguez de la Vega et al. 2004). From a structural point of view, insect defensins can be divided into two distinct subdomains comprising a conformationally flexible amino-terminal loop (n-loop) followed by a CSαβ scaffold shared with α-KTxs, both stabilized by three conserved disulfide bridges (Cornet et al. 1995).

Recently, "neofunctionalization" has been proposed to explain the origin of scorpion toxins from CSαβ-type defensins (Froy and Gurevitz 2004; Fry et al. 2009); however, it remains unsolved how such an event occurred. To address this question, one approach is to find surrogates of evolutionary intermediates connecting the two families, which can be tested in laboratory for structural and functional studies. In this work, we firstly analyzed the α-KTx family sequences to extract the conserved amino acid sites associated with structure and function (herein called "scorpion toxin signature" [STS]) and then searched for the insect defensins containing a STS to carry out experimental studies. The results show that a "STS"-containing insect defensin can structurally and functionally convert to an α-KTx-like neurotoxin through a single genetic deletion event, which provides first direct evidence that the sequence space of some venomous insect defensins can harbor the structure and function of α-KTxs, and thus suggests their evolutionary intermediate position in linking insect defensins and scorpion α-KTxs.

Results

The Signature of α-KTxs Associated with Structure and Function

By using WebLogo, we built the sequence logo of α-KTxs and identified eight structurally and functionally important residues conserved across the family as STS, in which six cysteines are involved in three disulfide bridges and two amino acids (Lys and Asn) in a four-residue long motif around the fourth cysteine (Lys-Cys4-Xaa-Asn) (Xaa, any amino acid) are key functional residues of α-KTxs (fig. 1). Mutations at these two sites (Lys^{27} and Asn^{30}) had the largest destabilizing effects on binding of agitoxin2 (AgTx2), an α-KTx isolated from the venom of the scorpion *Leiurus quinquestriatus hebraeus*, to the *Shaker* K^+ channel in *Drosophila* (Garcia et al. 1994; MacKinnon et al. 1998). This is consistent with a toxin-channel complex model derived from solid-state nuclear magnetic resonance (NMR) studies where the side chains of Asn^{30} on the toxin kaliotoxin (KTX) and Asp^{64} on the pore helix of one chain of KcsA-K_v1.3 (structurally equivalent to Asp^{431} of *Drosophila melanogaster Shaker* K^+ channel or Asp^{361} of rat K_v1.1) are predicted to form hydrogen bonds, whereas side chains of Lys^{27} directly enter into the pore region to contact the backbone carbonyls of Tyr^{78} on the channel filter (structurally equivalent to Tyr^{445} of *D. melanogaster Shaker* K^+ channel or Tyr^{375} of rat K_v1.1) (Lange et al. 2006). The functional importance of these two residues was also identified in a recent crystal structure of a K_v channel in complex with an α-KTx (CTX) though in this complex the location of the Asn slightly differs from the NMR-based complex model (Lange et al. 2006; Banerjee et al. 2013).

Hemipteran and Hymenopteran Defensins Possessing the Signature of α-KTxs

Given that the sequence of a gene often carries potential information for the evolution of new functions (Hall and Malik 1998), the recognition of STS in insect defensins would reveal candidates suitable for experimental testing the evolutionary potential of these molecules. To do this, we analyzed insect defensins derived from six insect orders (Coleoptera, Diptera, Hemiptera, Hymenoptera, Lepidoptera, and Phthiraptera) (fig. 2*A*; supplementary fig. S2, Supplementary Material online), from which a total of six insect species (i.e., *Notonecta glauca*, *Palomena prasina*, *Podisus maculiventris*, *N. vitripennis*, *N. girault*i, and *N. longicornis*) belonging to two venomous insect orders (Hemiptera and Hymenoptera) were found to possess defensins with a STS comprising six cysteines and two functional residues (Lys and Asn) at the four-residue long motif structurally equivalent to α-KTxs (fig. 2*B*). Given a distant phylogenetic relationship between Hemiptera and Hymenoptera (Trautwein et al. 2012), as reflected by the molecular tree of insect defensins (fig. 2*A*), the evolution of STS in defensins between the two venomous insect orders could be a convergent consequence. There are two groups of insect defensins in the parasitoid wasp *N. vitripennis*, in which the STS-containing members are categorized into the second group that contains three members (navidefensin2-1 to navidefensin2-3) (Gao and Zhu 2010). By using RT-PCR, we have isolated their cDNAs in adults and the cDNA of *navidefensin2-2* in the venom gland (fig. 2*C*).

Steric Hindrance of Insect Defensins in Peptide-Channel Interactions

As mentioned previously, in comparison with α-KTxs, insect defensins have a conformationally flexible n-loop (Cornet et al. 1995) (figs. 2*B* and 3*A*). The functional importance of this region in antimicrobial activity has been recognized by truncation (Ceřovský et al. 2011) and by designing hybrid defensins (Landon et al. 2008). Transferred cross-saturation experiments combined with site-directed mutagenesis highlighted at least six residues located in this region that are implicated in direct interaction with bacterial membranes (Takeuchi et al. 2004). However, the n-loop obviously hampers binding of a defensin to K_v channels since when an insect defensin is placed on the pore region of rat K_v1.1 with identical orientation to α-KTxs (Garcia et al. 2001), a serious steric

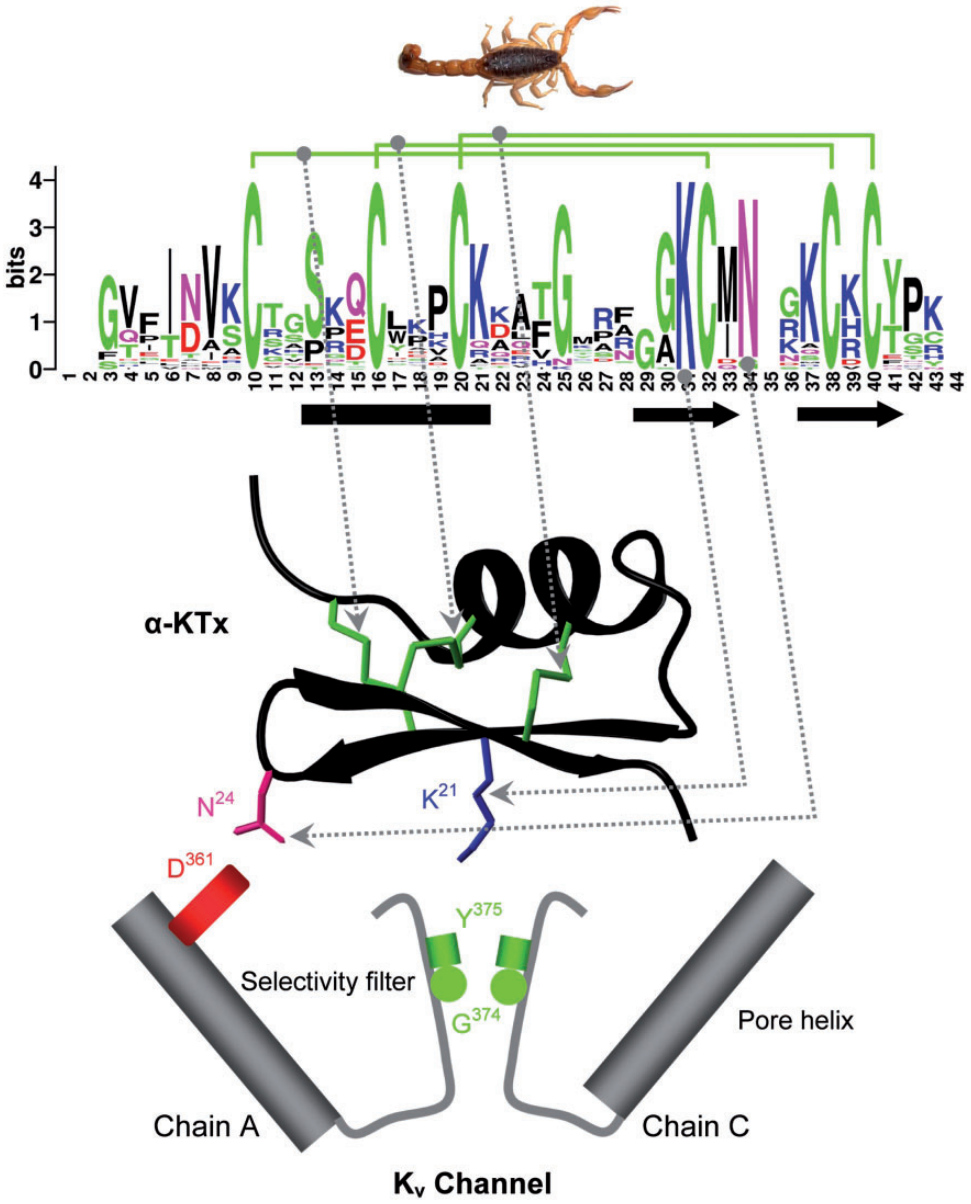

FIG. 1. The sequence logo of scorpion α-KTxs. A widely accepted toxin-channel interaction model accounts for the evolutionary conservation of residues in the interface: Lys^{21} and Asn^{24} (numbered according to CoTx1) in α-KTxs; Asp^{361}, Gly^{374}, and Tyr^{375} in K_v channels (numbered according to rat K_v1.1). Secondary structure elements and disulfide bridges of CoTx1 are extracted from its NMR coordinates (pdb entry 1PJV). A ribbon diagram, displayed by MOLMOL (Koradi et al. 1996), showing the signature of α-KTxs in stick representation.

hindrance occurs between the n-loop of the defensin and the turret of one chain of the channel (fig. 3*B*). These analyses not only provide structural basis for functional differences between α-KTxs and insect defensins but also indicate that a defensin with the motif Lys-Cys4-Xaa-Asn likely transforms into a toxin when its n-loop is deleted to remove the steric hindrance.

Structural Alteration from an Insect Defensin to an α-KTx

To confirm the hypothesis mentioned earlier, we selected navidefensin2-2 for further experimental study not only because it contains STS but also because it has been recruited into the venom gland (fig. 2*C*). In reference to cobatoxin 1 (CoTx1), a classical α-KTx of 32 residues isolated from the scorpion *Centruroides noxius* venom that blocks K_v1.1 channels with nanomolar affinity (Jouirou et al. 2004), we experimentally deleted the n-loop of navidefensin2-2 (^{5}VLSFQSKWVSPN^{16}) and designated this mutant molecule navitoxin (figs. 2*B* and 4*A*).

Navitoxin in its reduced form was chemically synthesized and its oxidized form with three disulfide bridges was obtained in an alkaline environment. The oxidized product was eluted later than the synthetic peptide on a C_{18} column, with a retention time (T_R) of 18.2 min (fig. 4*B*). Oxidized navitoxin had an experimental molecular mass of 3,267.0 Da, as determined by MALDI-TOF MS (fig. 4*C*), which

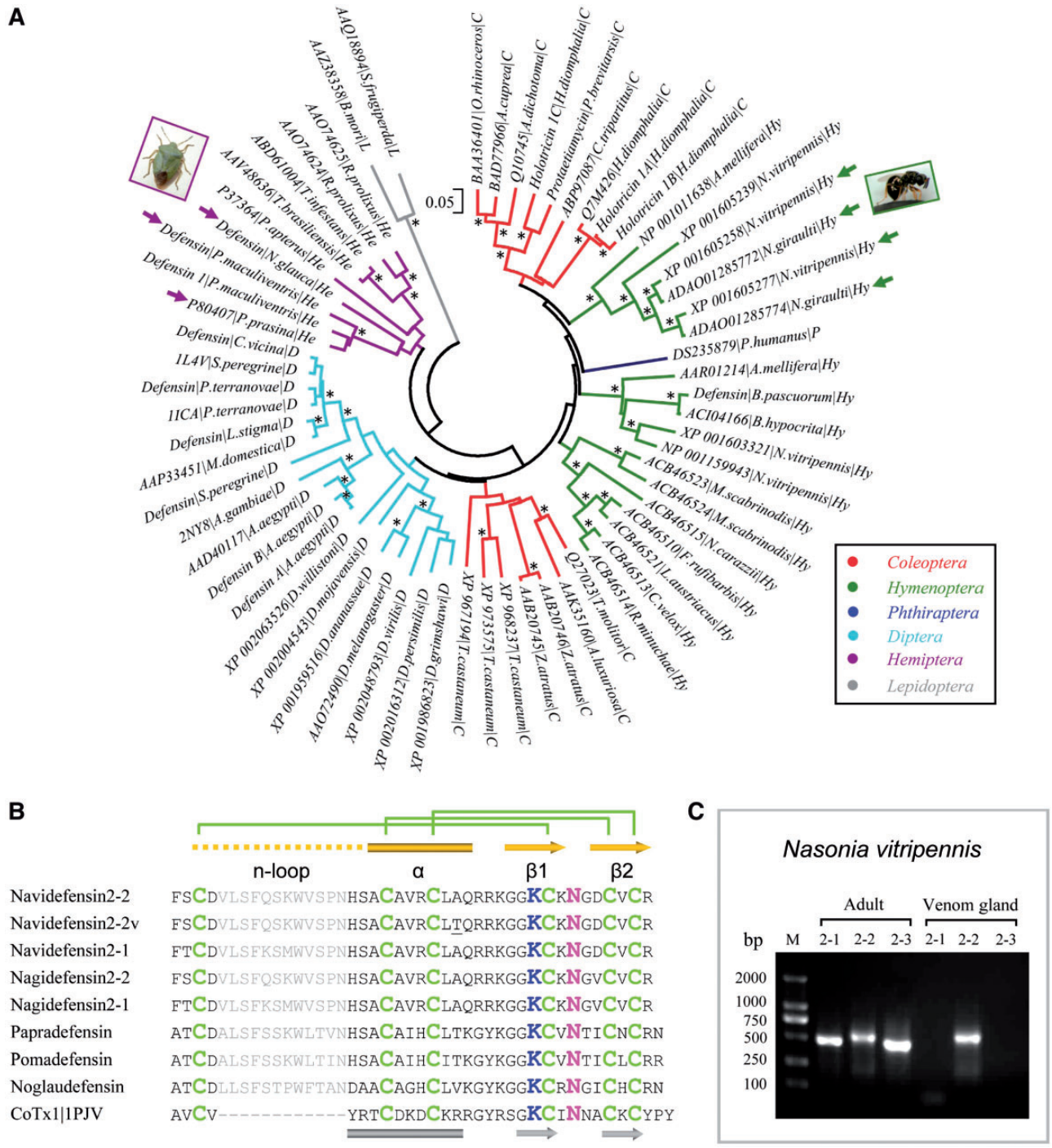

Fig. 2. Insect defensins. (*A*) An NJ tree showing positions of the STS-containing defensins (indicated by arrows). The scale bar indicates total amino acid divergence. Asterisks mark nodes that are supported by >50% bootstrap values. An ML tree with similar topology to the NJ tree is provided in supplementary figure S3, Supplementary Material online. (*B*) MSA of insect defensins with STS highlighted in color. The absence of the n-loop in α-KTxs (CoTx1 as a representative) is indicated by gaps. The conserved secondary structure elements and disulfide bridges in insect defensins (Dimarcq et al. 1998) are shown at the top of the alignment, and the structurally equivalent elements in α-KTxs, extracted from CoTx1, are shown at the bottom. Navidefensin2-2v is a polymorphic sequence of navidefensin2-2 with a point mutation (underlined), whose cDNA was cloned from the *N. vitripennis* venom gland. (*C*) RT-PCR detecting the expression of *navidefensin2-1* to *navidefensin2-3* in adults and the venom gland.

perfectly matches its theoretical mass of 3,266.8 Da (supplementary table S1, Supplementary Material online), indicating that its three disulfide bridges have been formed during in vitro folding.

The solution structure of navitoxin was solved with NMR-derived distance, hydrogen bond, and dihedral constraints. A summary of nuclear Overhauser effect (NOE) data is presented in figure 4*D*. From 100 calculated structures, we finally selected 20 with lower target function values and good structural and energetic statistics (fig. 4*E*; supplementary table S2, Supplementary Material online). The atomic root-mean-square deviation (RMSD) values of the mean coordinate

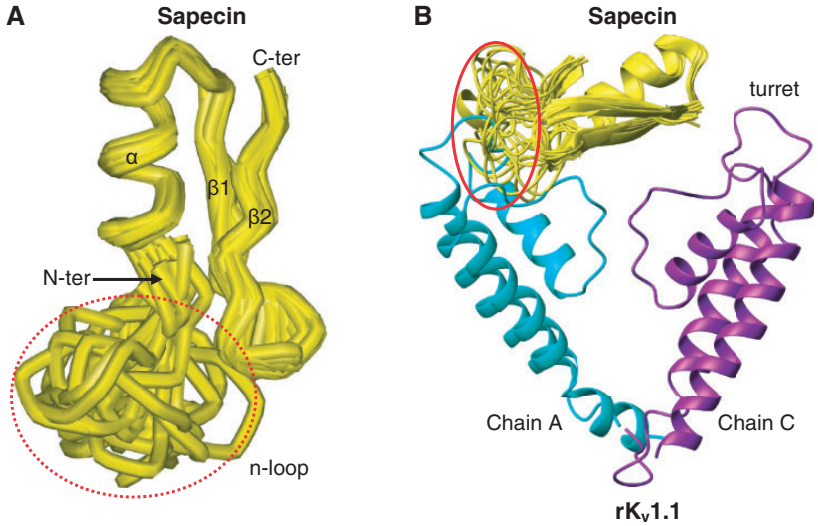

FIG. 3. Steric hindrance of insect defensins for interaction with K_v channels. (*A*) A family of 18 conformers of sapecin (pdb entry 1L4V) revealing conformational flexibility of the n-loop in insect defensins. (*B*) Steric hindrance between the n-loop of sapecin and the chain A turret of the channel $rK_v1.1$ is circled in red.

positions of navitoxin were 0.33 ± 0.13 Å for the backbone atoms from residues 2–29 and 0.86 ± 0.10 Å for all heavy atoms from residues 2–29, indicating an overall rigid structure that could facilitate key residues in a suitable conformation to interact with the channel pore, as in the case of other α-KTxs (MacKinnon et al. 1998; Lange et al. 2006). There are no violations in both distance and dihedral restraints, with 78.6% of the residues falling within the most favored regions of the Ramachandran plot and 21.4% within additional allowed regions. A ribbon representation of the secondary structures of navitoxin is shown in figure 4*F*, which presents a typical CSαβ fold stabilized by three disulfide bridges (Cys^3-Cys^{22}, Cys^8-Cys^{27}, and Cys^{12}-Cys^{29}).

Analysis of the navitoxin structure with STRIDE (Heinig and Frishman 2004) identified one α-helix spanning residues His^5 to Ala^{14} and two anti-parallel β-strands consisting of residues Gly^{20} to Ly^{23} and Asp^{26} to Cys^{29}. Superimposition of navitoxin and CoTx1 revealed a 1.05 Å of RMSD over 30 Cα atoms (fig. 4*F*), indicative of high structural similarity between them. Half of the surface of navitoxin is hydrophobic, and the rest has positive charges contributed by seven cationic residues (Arg^{11}, Arg^{16}, Arg^{17}, Lys^{18}, Lys^{21}, Lys^{23}, and Arg^{30}), with only two negatively charged residues exposed on the molecular surface (Asp^4 and Asp^{26}) (fig. 4*G*).

Peptide-Channel Complex Model Suggesting Putative Function of Navitoxin

As shown in figure 4*G*, two key STS residues (Lys^{21} and Asn^{24}) are fully exposed on the molecular surface of navitoxin, which constitutes a prerequisite to block a K^+ channel pore. A complex model between navitoxin and $rK_v1.1$ (fig. 5) can be compared with that of KTX-KcsA-$K_v1.3$ (Lange et al. 2006), in which Lys^{21} of navitoxin (Lys^{27} in KTX) is predicted to be close to Tyr^{375} of the channel filter (Tyr^{78} in KcsA-$K_v1.3$) and Asn^{24} (Asn^{30} in KTX) close to Asp^{361} of the pore helix (Asp^{64} in KcsA-$K_v1.3$), hinting their functional importance. This model also predicts that Lys^{18} of navitoxin (Arg^{24} in KTX) possibly binds to Asp^{361} of another chain of $rK_v1.1$ through electrostatic bonding, as observed in other toxin-channel interactions (Hidalgo and MacKinnon 1995; Lange et al. 2006) (supplementary fig. S4, Supplementary Material online). In this model, the n-loop-mediated steric hindrance has been thoroughly removed (fig. 5). All these observations suggest that navitoxin could possess a putative channel-blockade function.

Navitoxin Is a Typical K_v Channel Blocker

To study the functional consequence of the n-loop deletion, we compared electrophysiological effects of navitoxin and navidefensin2-2 (Gao and Zhu 2010) on four K_v channel isoforms ($K_v1.1$–$K_v1.4$). As expected, the defensin was inactive on these channels at 5 μM owing to the steric hindrance between the peptide and the channels. In contrast, navitoxin selectively inhibited the currents of $K_v1.1$–$K_v1.3$ at the same concentration, with larger effect on $K_v1.1$ and $K_v1.3$ (fig. 6). The IC_{50} (half maximal inhibitory concentration) values for these two channels are 529.3 ± 31.5 nM and 2,900.6 ± 125.3 nM, respectively (fig. 7*A*). The affinity of navitoxin on $K_v1.1$ is comparable with that of CoTx1 (500 nM) and 2-fold higher than CoTx2 (1,000 nM), a highly similar α-KTx to CoTx1 (Selisko et al. 1998; Jouirou et al. 2004), and 150-fold higher than PBTx3, a natural α-KTx from the venom of the scorpion *Parabuthus transvaalicus* (Huys et al. 2002). The K_v channel-blocking activity of navitoxin is also stronger than scorpion venom-derived KTxs with other folds, such as peptides with a CSαα fold, κ-KTxs with two helical segments, and the peptide with an inhibitor cysteine knot motif, most of which block K_v channels only at high micromolar concentrations (40–200 μM) (Srinivasan et al. 2002; Saucedo et al. 2012; Gao et al. 2013). Navitoxin exhibited no activity on other K_v channels ($K_v1.5$, $K_v1.6$, *Shaker*, $K_v2.1$, $K_v3.1$, $K_v4.2$, $K_v4.3$, and

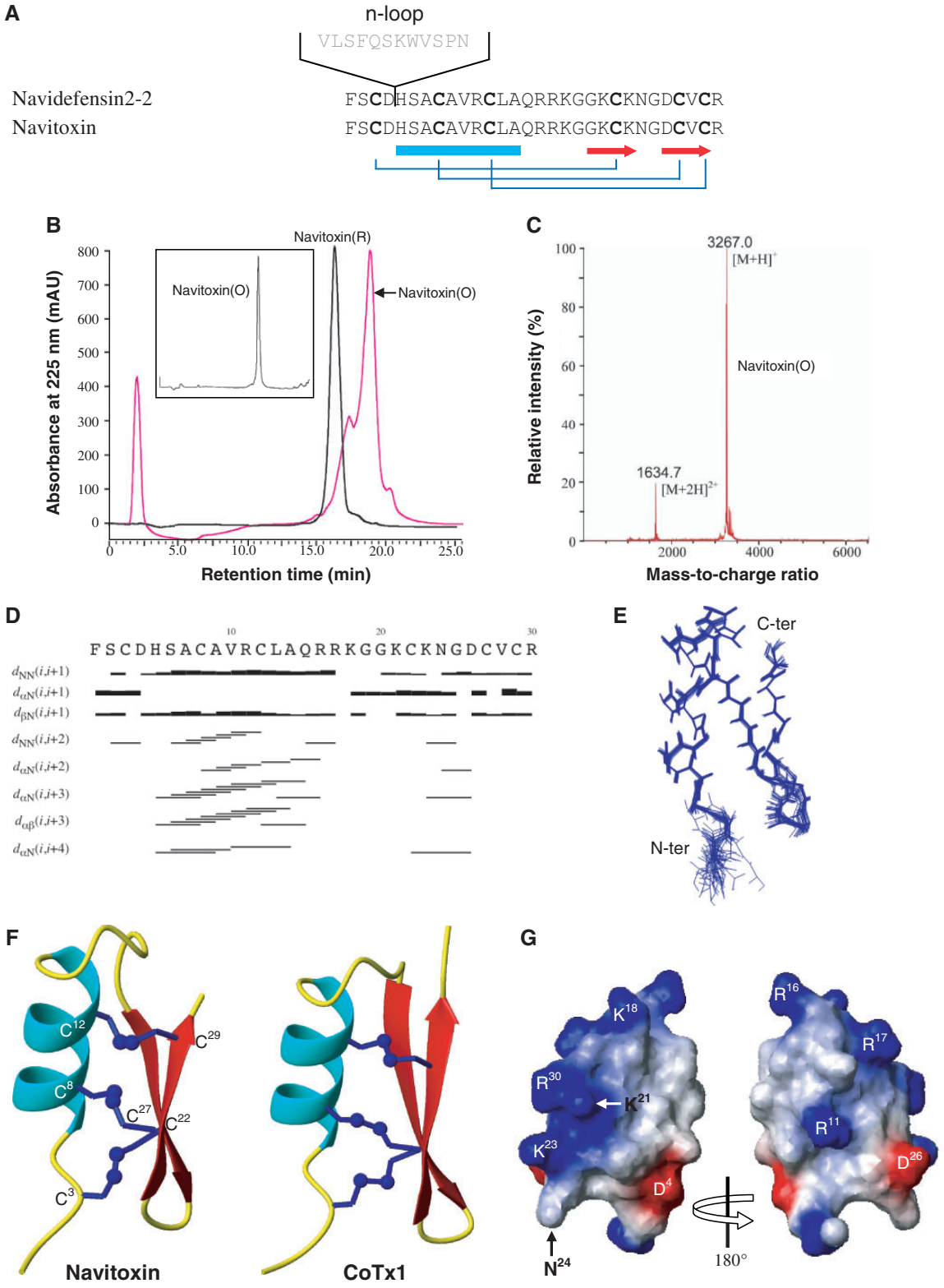

Fig. 4. Evolution-guided design of navitoxin. (*A*) Amino acid sequences of navidefensin2-2 and navitoxin. The deleted n-loop sequence is shown in gray. Secondary structure elements and disulfide bridges are extracted from the solution structure of navitoxin. (*B*) Oxidative refolding of navitoxin. Reversed-phase high-pressure liquid chromatography (RP-HPLC) showing retention time (T_R) difference between the reduced and oxidized form. O, oxidized (red); R, reduced (black). Inset, repurification of navitoxin to remove the minor components produced during refolding process. (*C*) MALDI-TOF MS of the refolded peptide. (*D*) Summary of NOE data. The thickness of the bars indicates the intensity of the NOEs. (*E*) A family of 20 lowest energy structures superimposed over the backbone atoms of residues 2–29. (*F*) A ribbon representation with disulfide connectivities are shown in ball-and-stick format by MOLMOL (Koradi et al. 1996). The cysteine positions are labeled by their residue numbers. For comparison, the structure of CoTx1 is also shown here. (*G*) Electrostatic potential map of navitoxin. Red, blue, and gray represent negatively charged, positively charged, and electrostatically neutral zones, respectively.

hERG) at 5 μM (supplementary fig. S5, Supplementary Material online).

The blockade of $K_v1.1$ by navitoxin occurred rapidly, and binding was reversible upon washout (fig. 7*B*). In ND96 solution, this peptide inhibited the currents of $K_v1.1$ at the test potentials from −40 to + 80 mV, and the inhibition was not associated with a change of the shape of the current–voltage (*I*–*V*) relationship (fig. 7*C*). In this solution, the $V_{1/2}$ of the control and in the presence of 1 μM peptide was characterized by a value of −14.47 ± 1.16 mV ($n = 4$) and −12.09 ± 3.40 mV ($n = 5$), respectively. No significant shift was observed. In high K^+ solution, it can be seen that navitoxin does not significantly alter the reversal potential (fig. 7*D*). All these data indicate that like α-KTxs, navitoxin acts as a typical K^+ channel blocker. The emergence of toxicity in navitoxin is accompanied by complete loss of antimicrobial activity to *Micrococcus luteus* and 4-fold reduction to *Bacillus megaterium* when compared with navidefensin2-2 (Gao and Zhu 2010) (supplementary table S3, Supplementary Material online) due to the deletion of the functionally important n-loop (Takeuchi et al. 2004; Landon et al. 2008; Ceřovský et al. 2011).

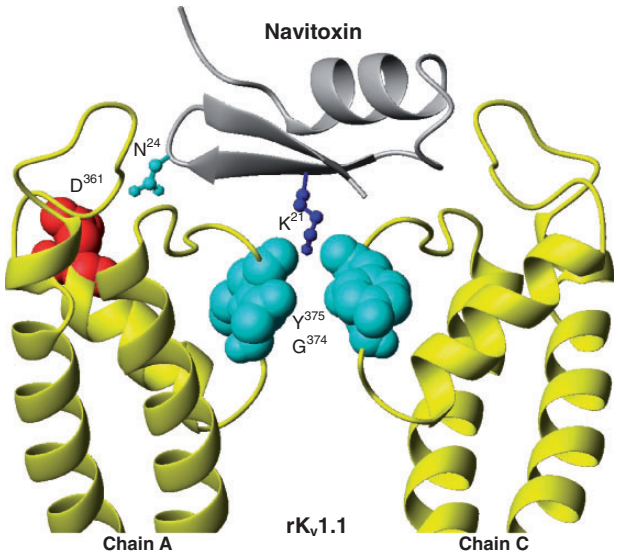

FIG. 5. A model of the navitoxin-r$K_v1.1$ complex. Residues presumably involved in binding include Lys^{21} and Asn^{24} in navitoxin (indicated in a ball-and-stick model), and Asp^{361}, Tyr^{375}, and Gly^{374} in r$K_v1.1$ (shown in a space-filled model).

Navitoxin Binds to K_v Channels in the Same Manner as α-KTxs

To confirm the functional role of STS in navitoxin, we chemically synthesized its two mutants (K21A and N24A) (supplementary table S1 and fig. S6, Supplementary Material online) and studied effects of the mutations on $K_v1.1$–$K_v1.3$ (fig. 8*A*). Consequently, we found that K21A was almost inactive on all the channels initially sensitive to navitoxin when a high concentration of peptide (5 μM) was applied. At the same concentration, it was found that N24A was a bit less active on $K_v1.1$ and inactive on the two other channels tested. The loss or decrease of the activity in these two mutants is consistent with the data from AgTx2 and other α-KTxs (Ranganathan et al. 1996; MacKinnon et al. 1998; Garcia et al. 2001; Lange et al. 2006). Regarding the residual activity of N24A on $K_v1.1$, one possibility is that the mutation could be complemented by the adjacent Lys^{23} through electrostatic interaction with Asp^{361} of the channel (fig. 5). Further substitution of the key Lys in navitoxin with Arg (K21R) resulted in nearly complete loss of the activity on $K_v1.1$–$K_v1.3$ (fig. 8*A*). These observations suggest that Lys^{21} and Asn^{24} fulfill similar functional roles as their α-KTx counterparts.

To rule out a possible structural role of these mutations, we undertook comparative structural analysis of these mutants by circular dichroism (CD) spectroscopy (Kelly and Price 2000). As shown in figure 8*B*, the mutants possess nearly

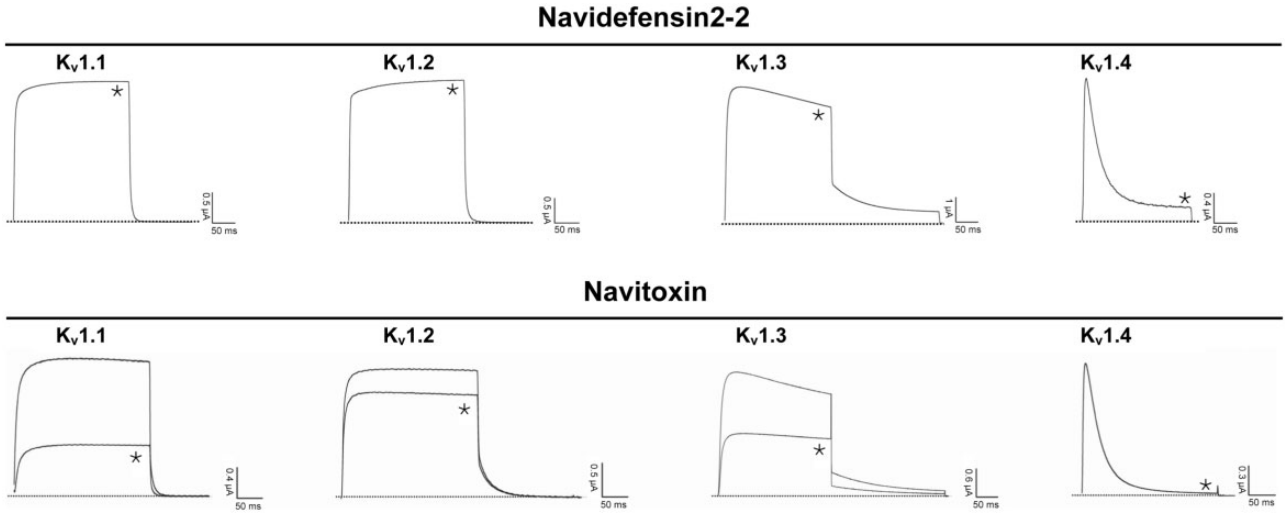

FIG. 6. Navitoxin, in contrast to navidefensin2-2, inhibits K_v channels expressed in *Xenopus* oocytes. Representative whole-cell current traces in control and peptide conditions are shown. The dotted line indicates the zero-current level. Asterisks mark steady-state current traces after application of 5 μM navidefensin2-2 or navitoxin. Traces shown are representative traces of at least three independent experiments ($n \geq 3$).

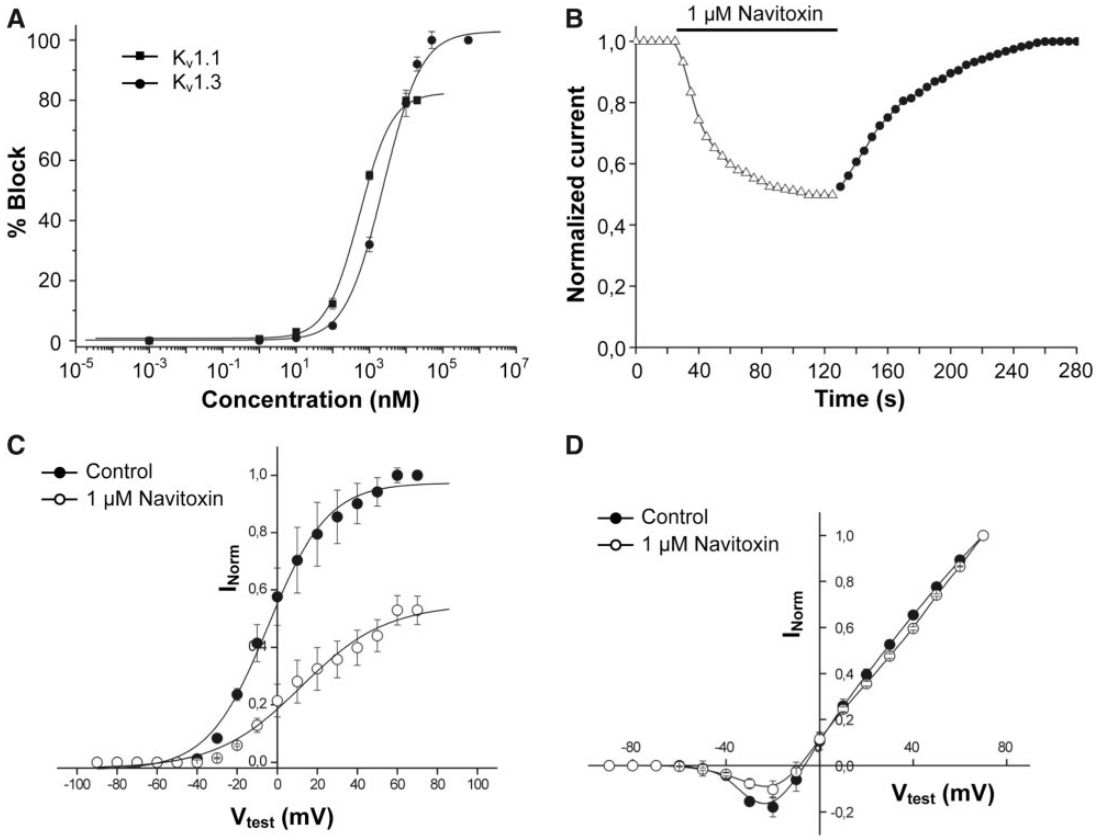

FIG. 7. Functional features of navitoxin on $K_v1.1$ and $K_v1.3$ channels. (*A*) Dose–response curve on $K_v1.1$ (squares) and $K_v1.3$ (circles) channels obtained by plotting the percentage blocked current as a function of increasing toxin concentrations. (*B*) Fast kinetics of inhibition of $K_v1.1$ channels and reversibility of the inhibition upon washout. Control (open triangles), wash-in (open triangles + black bar), and wash-out (closed circles). Values for τ_{on} and τ_{off} in this experiment were 21.13 ± 0.77 s and 52.32 ± 1.13 s, respectively. *I–V* curves of $K_v1.1$ in ND96 (*C*) and HK solutions (*D*).

identical CD spectra to navitoxin, as identified by large negative contributions between 207 and 225 nm and positive maximum values around 190 nm, indicating no structural changes by these mutations. The spectra observed here are also highly similar to those of CoTx1 (Jouirou et al. 2004), in agreement with their structural data presented in figure 4*F*. Our observations thus indicate that the functional loss or reduction of the mutants is a consequence of side-chain substitutions rather than structural alteration of the peptide. Taken together, these results demonstrate that navitoxin binds to K_v channels in the same manner with α-KTxs (Garcia et al. 2001; Lange et al. 2006).

Discussion

The restricted distribution of the STS-containing defensins in two venomous insect orders and the recruitment of *navidefensin2-2* into the venom gland suggest that these molecules might be of evolutionary potential (Hall and Malik 1998) in developing new components of insect venom similar to scorpion α-KTxs, in addition to their current function in providing protection against venom gland infection. In this work, we exploit the potential via experimental deletion of the n-loop of a venomous insect defensin leading to a typical α-KTx (navitoxin) with high affinity against K_v channels. Variations in the length of the n-loop are frequent within the CITD (supplementary fig. S2, Supplementary Material online). This is in line with the opinion that loops in an ancestral structure are targets for indel mutations during evolution (Pascarella and Argos 1992). In this case, extensive sequence divergence between defensins and toxins could be partly explained by the deletion inducing an increase in the substitution rate of their flanking regions (Tian et al. 2008) though accelerated evolution is still considered as a major factor (see later). Our work substantiates the functional significance of one small deletion in the emergence of a novel functional property of an effector molecule, conceptually first involved in innate immunity but later developed to target ion channels of prey and competitors.

Although the evolution of a K_v channel-targeted toxin from an antimicrobial insect defensin has been demonstrated experimentally, it does not necessarily follow that this is the way that the event actually happened, and that the insect defensins identified here are valid surrogates of the true evolutionary intermediates. However, high similarities between navitoxin and α-KTxs at the structural, functional, and mechanistic levels provide convincing evidence that venomous insect-derived defensins are valid surrogates of an evolutionary intermediate in linking defensins and α-KTXs. Because of the early origin and wide phylogenetic distribution of insect defensins ranging from fungi to amphioxus, it is reasonable to

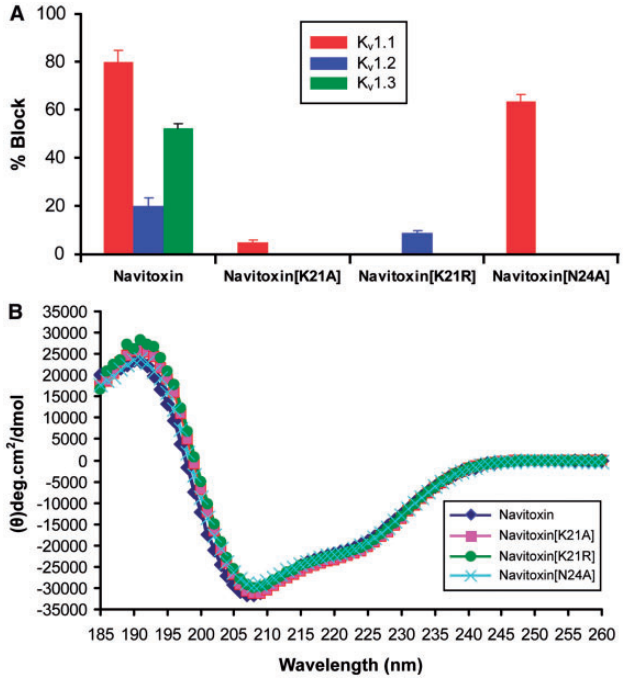

FIG. 8. Identification of functional importance of Lys^{21} and Asn^{24} in navitoxin by mutational analysis. (*A*) Comparison of blocking effects of navitoxin and mutants on three cloned K_v channels expressed in *Xenopus* oocytes. The peptide concentration used is 5 μM. (*B*) CD spectra of navitoxin and its mutants, recorded from 185 to 260 nm with a peptide concentration of 0.1 mg/ml in water.

infer that after scorpions diverged from other arthropods, an ancestral STS-containing defensin, similar to those identified here from the venomous insects (fig. 2*B*), could be firstly developed and subsequently converted into a toxin through a single genetic event (fig. 9).

Although the evidence remains scarce, with just a handful of scorpion species ever studied for defensins, no CITD has ever been described in scorpions (Cociancich et al. 1993; Ehret-Sabatier et al. 1996; Froy and Gurevitz 2004; Rodríguez de la Vega et al. 2004; Rendón-Anaya et al. 2012), as also recently confirmed by the analysis of the first complete genome of the scorpion *Mesobuthus martensii*, from which a total of six defensins were predicted, all belonging to ancient invertebrate-type defensins (AITDs) (Cao et al. 2013). In view of a paralogous relationship between CITDs and AITDs, both originated from an early gene duplication event preceding the animal and fungal split (Zhu 2008), the clear lack of navidefensin2-2-like CITDs in scorpions indicates that in the lineage this class of molecules could have diverged into α-KTxs following speciation, in favor of an ancestral paralogous relationship between scorpion AITDs and α-KTxs. There are two striking facts that exclude the possibility of scorpion AITDs as the ancestor of α-KTxs: 1) unlike CITDs that evolved fast with excess point mutations and insert/deletions (indels) in the n-loop, AITDs from fungi to animals evolved slowly (Charlet et al. 1996; Mygind et al. 2005; Zhu 2008; Zhu et al. 2012; Cao et al. 2013); 2) all the AITDs identified so far, including the six newly predicted defensins from the *Me. martensii* genome (Cao et al. 2013), lack a STS, implying that their

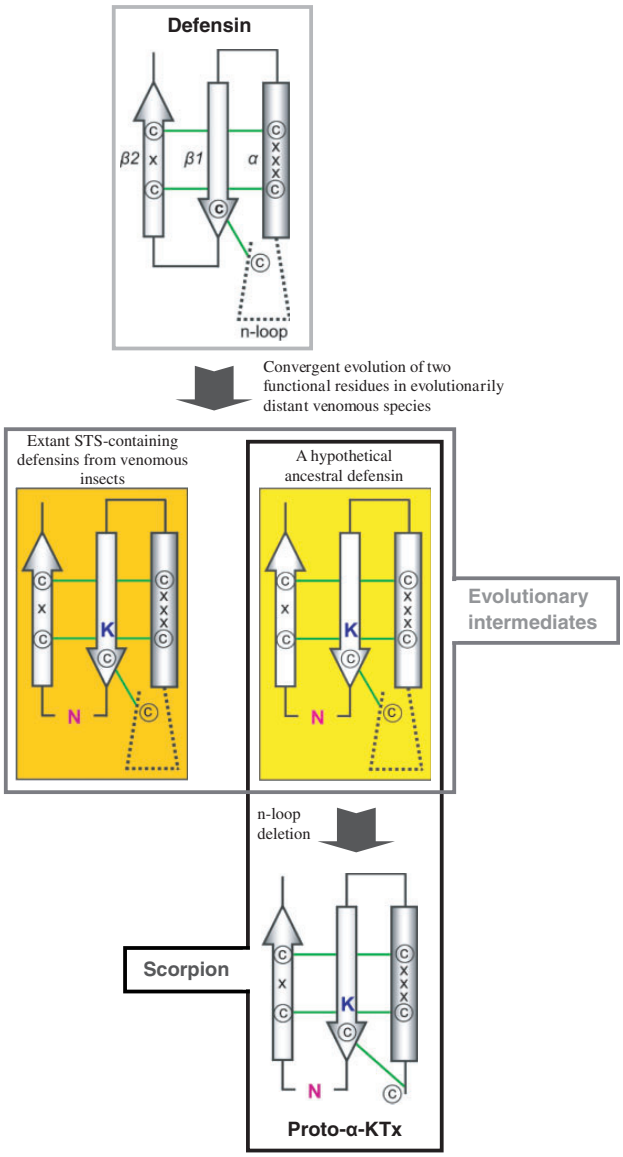

FIG. 9. Proposed evolutionary pathway for the origin of scorpion α-KTxs from an ancestral defensin. Evolutionary emergence of the two functional residues (Lys and Asn) followed by the n-loop deletion in the scorpion lineage is highlighted. The schematic picture of the CSαβ scaffold is modified from our previous work (Zhu et al. 2005). Evolutionary intermediates in different lineages are shadowed in golden or yellow, where the extant STS-containing defensins from venomous insects are considered as the surrogates of the "evolutionary intermediate" and the hypothetical ancestral scorpion defensin as the proposed true evolutionary intermediate.

sequence space does not harbor the structure and function of α-KTxs. On the contrary, some CITDs from venomous insects (e.g., navidefensin2-2) possess the features (evolutionary potential) to develop into a K^+ channel toxin. It is remarkable that with the exception of scorpion AITDs and α-KTxs, most of AITDs and CITDs from other species contain a propeptide located between the signal peptide and mature peptide (Froy et al. 1999; Froy and Gurevitz 2004; Zhu 2008; Cao et al. 2013) (supplementary fig. S1, Supplementary Material online), suggesting the genetic loss of a propeptide in the scorpion lineage.

By N- and C-terminal deletions of scorpion toxins affecting voltage-gated Na^+ channels (Na_vTxs), Cohen et al. (2009) generated two miniature peptides with sequence, structural, and functional similarities to drosomycin, a classical CSαβ-type antifungal peptide initially identified from *Drosophila* (Fehlbaum et al. 1994) and later extensively found in Ecdysozoa (including Arthropoda, Nematoda, and Tardigrada) (Zhu and Gao 2014), suggesting that the deletions release their ancestral function. This is highly consistent with the observation that toxins evolved from proteins of physiological function often possess ancestral bioactivities (Fry 2005; Fry et al. 2009). Similarly, navitoxin, evolved from navidefensins2-2, also retains some weak antibacterial function (supplementary table S3, Supplementary Material online). When grafting the N-terminal turn and the C-tail of a scorpion Na_vTx to the drosomycin scaffold, Zhu et al. (2010) found that this engineered molecule obtained ability to target rat Na^+ channels. These studies highlight a putative role of the N-terminal insertion and C-terminal extension in the toxicity origin of scorpion Na_vTxs (Cohen et al. 2009; Zhu et al. 2010). Our results serve to further highlight how a small deletion can transform a functional defensin into a functional K_v channel blocker even when their sequences are substantially divergent. All these data imply that scorpion toxins targeting Na^+ and K^+ channels independently originated from different ancestors, one from an ancestral antifungal peptide and another from an ancestral antibacterial defensin. They represent two typical examples of divergent evolution where indel-mediated structural alterations in ancestral structural scaffolds led to functional shift of proteins from immunity against microbes to defense against competitors and prey capture. Intriguingly, some scorpion Na_vTxs were found to exhibit significant sequence similarity to drosomycin (*E* values from 7×10^{-4} to 5×10^{-8} obtained by BlastP search of the nr database of GenBank on December 21, 2013, by the precursor amino acid sequence of drosomycin as a query), whereas such similarity is not observed between scorpion α-KTxs and insect defensins. This might be a mirror of their target diversity because compared with the conserved Na^+ channel family (Goldin 2002), K^+ channels form a large superfamily of transmembrane proteins with enormous sequence divergence and high functional variability (Coetzee et al. 1999), which could drive the accelerated evolution of α-KTxs for adaptation of the alteration of their targets, as in the case of the *Conus* toxins (Duda and Palumbi 1999).

It is worth mentioning that the common presence of a phase-1 intron (an intron between the first and second bases of the codon) at the end of signal sequences has been long considered as evidence for evolution of all scorpion toxins with a CSαβ fold from an ancestral Lqdef-like AITD by gene duplication and divergence (Froy et al. 1999; Froy and Gurevitz 2004) despite their signal peptides lack sequence similarity (supplementary fig. S7, Supplementary Material online). However, it was recently found that some evolutionarily unrelated scorpion venom peptides with distinctive folds, such as linear α-helical AMPs and ICK-type toxins, also possess a phase-1 intron near the cleavage site of signal sequences (supplementary fig. S7, Supplementary Material online). Moreover, previous studies on human introns also revealed that a phase-1 intron near the cleavage site of signal sequences is a universal feature of many secretary proteins (Tordai and Patthy 2004), which led to the suggestion that exon shuffling may have played key roles in acquiring signal sequences for non-secretary proteins (Vibranovski et al. 2006). Therefore, opposite to the view of common origin of the intron among scorpion CSαβ-type peptides (Froy et al. 1999; Froy and Gurevitz 2004) is the scenario where this intron is a relic of exon shuffling involved in recruitment of genes encoding different proteins with physiological functions (e.g., antifungal drosomycin and antibacterial defensin, both implicated in immunity) into scorpion venom during evolution.

Conclusion and Perspectives

Although it has long been suggested that scorpion K^+ channel toxins and antibacterial defensins share a common evolutionary origin, very low sequence similarity brings a great challenge in establishing a convincing evolutionary link between them. On the basis of the "evolutionary intermediate" concept, we present for the first time a feasible solution for the old enigma using an experimental approach. We discovered that 1) removal of steric hindrance of peptide-channel interactions in an insect defensin structure results in a K_v channel-targeted neurotoxin, provided that 2) the defensin structure contains two crucial residues located in STS. Furthermore, when these two conditions are met, our study shows that an insect defensin-derived neurotoxin is capable of binding to K_v channels in the same manner as scorpion α-KTxs, which provides new evidence in favor of the predictability of toxicity evolution—arising via structural deletion of a loop on an ancestral defensin scaffold recruited into the venom to remove steric hindrance of peptide-channel interaction. The experimental strategy is the first employed to establish an evolutionary relationship of two distantly related peptide families and will also be applicable to the recognition of homology of other distantly related protein families. Our approach might be valuable in enlarging the library of neurotoxins from nontoxic peptide resources as molecular tools for studying the structure–function relationship of K^+ channels (MacKinnon et al. 1998; Dutertre and Lewis 2010) and in considering putative toxicity of insect defensin-derived drugs especially when assuming that n-loop deletion could occur in vivo by degradation.

Materials and Methods

Sequence and Structural Analysis

To construct the logo of α-KTxs, a total of 18 subfamilies containing 74 members (Rodriguez de la Vega and Possani 2004) were aligned by CLUSTAL (http://www.ebi.ac.uk/Tools/msa/clustalw2/, last accessed January 24, 2014). The multiple sequence alignment (MSA) was used to generate the logo by WebLogo, a web-based tool for creating sequence logos from MSA (Crooks et al. 2004). The model structure of $rK_v1.1$ was built by the project mode of the Swiss MODEL server (http://swissmodel.expasy.org/, last accessed January 24, 2014) from the experimental structure of $K_v1.2$ (pdb entry 2A79). The

complex model of navitoxin-rK$_v$1.1 was constructed based on Css20-hK$_v$1.3 (Corzo et al. 2008) according to the method previously described (Zhu et al. 2011).

Phylogenetic Tree Construction

Amino acid sequences of insect defensins derived from six insect orders were aligned by ClustalX (Supplementary fig. S2, Supplementary Material online), which were then used to construct a neighbor-joining (NJ) tree on the basis of the *p*-distance substitution model with pairwise deletion of gaps (MEGA 4.1) (Tamura et al. 2007). A maximum likelihood (ML) tree was also constructed on the basis of the Jones–Taylor–Thornton substitution model with a gamma distribution of rates between sites (MEGA 5.2) (Tamura et al. 2011). In ML analysis, an initial tree was first built automatically with the NJ/BioNJ methods and then variants of the topology were created with the nearest neighbor interchange method to search for topologies fitting the data better. Five hundred bootstrap replicates were performed in the NJ tree and the ML tree (Tamura et al. 2011).

cDNA Cloning

Total RNAs of *Nasonia vitripennis* adults or venom glands were prepared with Total RNA Isolation Reagent (BioTeke, Beijing, China). Reverse transcription from total RNAs to the first-strand cDNAs was performed using the EasyScript First-Strand cDNA Synthesis Kit (TransGen, Beijing, China) and a universal oligo(dT)-containing adaptor primer (dT3AP). Two rounds of PCR amplification were carried out by Taq DNA polymerase and two nested forward primers designed based on nucleotide sequences of signal peptide-coding regions of *navidefensin2-1* to *navidefensin2-3* (Gao and Zhu 2010) (NaviDef2-1F: ATGAAGGTCCTCGTGGCTCTC; NaviDef2-1Fn: CGCTAGTCGCCAGTGCTTAC; NaviDef2-2F: ATGAAGG TCCTCGTTGTTTTG; NaviDef2-2Fn: GCGCTGTTTTCGCCGG AGCT; NaviDef2-3F: ATGAAGTTCCTGACGGTTTTC; NaviDef2-3Fn: AGTCGCCAGTGCTTACGGAG), and the universal reverse primer 3AP (Gao and Zhu 2010). PCR products were ligated into pGM-T, and resultant recombinant plasmids were transformed into *Escherichia coli* DH5α. Recombinant clones were sequenced through the chain termination method using the T7 primer. Nucleotide sequences of *navidefensin2-1*, *navidefensin2-2*, *navidefensin2-2v*, and *navidefensin2-3* have been deposited in the GenBank database (http://www.ncbi.nlm.nih.gov/, last accessed January 24, 2014) under accession numbers of JQ617291, JQ617292, JQ661327, and JQ617294.

Chemical Synthesis and Oxidative Refolding

Navitoxin and its mutants K21A, K21R, and N24A were chemically synthesized in their reduced form by ChinaPeptides Co., Ltd. (Shanghai, China). For oxidative refolding, peptide samples were dissolved in 0.1 M Tris-HCl buffer (pH 8.0) to a final concentration of 1 mM and incubated at 25 °C for 48 h. The peptides were purified to homogeneity by reversed-phase high-pressure liquid chromatography. Purity and molecular mass of these peptides were determined by matrix-assisted laser desorption ionization time-of-flight mass spectrometry (MALDI-TOF MS) on a Kratos PC Axima CFR plus (Shimadzu Co. Ltd., Kyoto, Japan).

CD Spectroscopy

The CD spectra of navitoxin, K21A, K21R, and N24A were recorded on Chirascan-plus CD spectrometer (Applied Photophysics Ltd., UK). Spectra were measured at room temperature from 260 to 185 nm using a quartz cell of 1.0 mm thickness. Data were collected at 1 nm intervals with a scan rate of 60 nm/min. CD spectra measurements are an average of three scans. Data are expressed as mean residue molar ellipticity (θ).

NMR Structural Analysis

The purified navitoxin (2.0 mg) was dissolved in 300 µl H_2O containing 10% D_2O for the NMR lock, and the sample pH was adjusted to 3.0 with direct reading of a pH meter. After a series of NMR measurements, the sample was lyophilized and then dissolved in 100% D_2O at pH 3.0 for another set of NMR experiments. Slowly exchanging amide protons suggesting the formation of hydrogen bonds were identified in NMR data of the fresh D_2O sample. All NMR data at 298 K were recorded on a Bruker Avance III 800 spectrometer equipped with a triple-resonance TCI-cryogenic probe. For both samples, we recorded the two-dimensional NMR data, TOCSY using 70 ms spin lock time (Bax and Davis 1985) and NOESY with 200 ms mixing time (Jeener et al. 1979). All FID data were processed with NMRPipe (Delaglio et al. 1995) and analyzed with SPARKY (Goddard and Kneller 2004). The three-dimensional structure of navitoxin was calculated with CYANA ver. 2.1 (López-Méndez and Güntert 2006). The structural quality was evaluated with procheck-NMR (Laskowski et al. 1996). The structural figures were generated with MOLMOL (Koradi et al. 1996). The chemical shift data and coordinates of navitoxin were deposited to Biological Magnetic Resonance Data Bank (accession number 11535) and Protein Data Bank (accession number 2RTY), respectively.

Expression of Voltage-Gated Ion Channels in *Xenopus* Oocytes

For the expression of the K$_v$ channels (rK$_v$1.1, rK$_v$1.2, hK$_v$1.3, rK$_v$1.4, rK$_v$1.5, rK$_v$1.6, *Shaker* IR, rK$_v$2.1, hK$_v$3.1, rK$_v$4.2, rK$_v$4.3, and hERG) in *Xenopus* oocytes, the linearized plasmids were transcribed by the T7 or SP6 mMESSAGE-mMACHINE transcription kit (Ambion, USA). The harvesting of stage V–VI oocytes from anesthetized female *Xenopus laevis* frogs was described previously (Liman et al. 1992). Oocytes were injected with 50 nl of cRNA at a concentration of 1 ng/nl using a microinjector (Drummond Scientific, USA). The oocytes were incubated in ND96 (in mM): NaCl, 96; KCl, 2; $CaCl_2$, 1.8; $MgCl_2$, 2; and HEPES, 5 (pH 7.4), supplemented with 50 mg/l gentamycin sulfate.

Electrophysiological Recordings

Two-electrode voltage-clamp recordings were performed at room temperature (18–22 °C) using a Geneclamp

500 amplifier (Molecular Devices, USA) controlled by a pClamp data acquisition system (Axon Instruments, USA). Whole cell currents from oocytes were recorded 1–4 days after injection. The bath solution is ND96. Voltage and current electrodes were filled with 3 M KCl. Resistances of both electrodes were kept between 0.5 and 1.5 MΩ. The elicited currents were sampled at 1 kHz and filtered at 0.5 kHz with a four-pole low-pass Bessel filter. Leak subtraction was performed using a P/4 protocol. $K_v1.1$–$K_v1.6$ and *Shaker* currents were evoked by 500 ms depolarizations to 0 mV followed by a 500 ms pulse to −50 mV, from a holding potential of −90 mV. Current traces of hERG channels were elicited by applying a + 40 mV prepulse for 2 s followed by a step to −120 mV for 2 s. $K_v2.1$, $K_v3.1$ and $K_v4.2$, $K_v4.3$ currents were elicited by 500 ms pulses to + 20 mV from a holding potential of −90 mV.

To investigate the current–voltage relationship, current traces were evoked by 10 mV depolarization steps from a holding potential of −90 mV. To assess the concentration dependency of the toxin induced inhibitory effects, a concentration–response curve was constructed, in which the percentage of current inhibition was plotted as a function of toxin concentration. Data were fitted with the Hill equation: $y = 100/[1 + (IC_{50}/[\text{toxin}])^h]$, where y is the amplitude of the toxin-induced effect, IC_{50} is the toxin concentration at half-maximal efficacy, [toxin] is the toxin concentration, and h is the Hill coefficient. To investigate the bimolecular kinetics of toxin inhibition, oocytes expressing $K_v1.1$ channels were depolarized to 0 mV for 0.5 s from a holding potential of −90 mV every 5 s, both in the absence and presence of different concentrations of toxin. The obtained current values were plotted as a function of time. Data were fitted with the following exponential equation: $y = Ae^{-t/\tau}$, where t represents the time, A is the amplitude of the current, and τ is the time constant for toxin binding (τ_{on}) or toxin unbinding (τ_{off}). The first-order association rate constant (k_{on}) was calculated using following equation: $\tau_{on} = (k_{on} + k_{off})^{-1}$. The first-order dissociation constant (k_{off}) was calculated using the equation: $\tau_{off} = {k_{off}}^{-1}$. Two sample means were compared using a paired Student's t-test ($P < 0.05$). All data represent at least three independent experiments ($n \geq 3$) and are presented as mean ± standard error.

Antimicrobial Assays

Antimicrobial activity of peptides was evaluated by the inhibition zone assay, as described previously (Gao and Zhu 2010). Microbial strains used here include *M. luteus* and *B. megaterium*, two Gram-positive bacteria sensitive to navidefensin2-2, and *E. coli* and *Salmonella typhimurium*, two Gram-negative bacteria resistant to navidefensin2-2 (Gao and Zhu 2010).

Supplementary Material

Supplementary tables S1–S3 and figures S1–S7 are available at *Molecular Biology and Evolution* online (http://www.mbe.oxfordjournals.org/).

Acknowledgments

S.Z. designed the research and performed all evolutionary and structural biology analyses. B.G., S.P., and Y.U. did the biochemical, molecular, electrophysiological, and structural studies. S.Z., S.O., and J.T. wrote the paper. All authors reviewed, revised, and approved the manuscript. The authors are grateful to Prof. L.D. Possani for critical reading of the manuscript and two anonymous reviewers for valuable comments. They thank Prof. O. Pongs for providing cDNAs for $rK_v1.1$, $rK_v1.2$, $rK_v1.4$, $rK_v1.5$, and $rK_v1.6$ channels. The $hK_v1.3$ clone was kindly provided by Prof. M.L. Garcia, *Shaker* IR by Prof. G. Yellen, and the hERG clone by Prof. M. Keating. The $hK_v3.1$, $rK_v4.2$, and $rK_v4.3$ clones were kindly provided by Prof. D.J. Snyders. The authors (Y.U. and S.O.) thank all technical staffs at Center for Nano Materials and Technology (CNMT), Japan Advanced Institute of Science and Technology (JAIST), for their assistance to maintain the NMR magnet used in this study. CNMT, JAIST, is also acknowledged for the financial support to maintain the NMR machine. This work was supported by the National Natural Science Foundation of China (31221091) and the National Basic Research Program of China (2010CB945300) to S.Z. and G.0257.08 and G.0433.12 (F.W.O.-Vlaanderen), OT-12-81 (K.U. Leuven), P7/10 (Interuniversity attraction Poles Program-Belgian State-Belgian Science Policy), and BIL 07/10 (China) to J.T.

References

Bax A, Davis DG. 1985. MLEV-17-based two-dimensional homonuclear magnetization transfer spectroscopy. *J Magn Reson.* 65:355–360.

Banerjee A, Lee A, Campbell E, Mackinnon R. 2013. Structure of a pore-blocking toxin in complex with a eukaryotic voltage-dependent K^+ channel. *Elife* 2:e00594.

Bontems F, Roumestand C, Gilquin B, Menez A, Toma F. 1991. Refined structure of charybdotoxin: common motifs in scorpion toxins and insect defensins. *Science* 254:1521–1523.

Brodie ED. 2009. Toxins and venoms. *Curr Biol.* 19:R931–R935.

Cao Z, Yu Y, Wu Y, Hao P, Di Z, He Y, Chen Z, Yang W, Shen Z, He X, et al. 2013. The genome of *Mesobuthus martensii* reveals a unique adaptation model of arthropods. *Nat Commun.* 4:2602.

Ceřovský V, Slaninová J, Fučík V, Monincová L, Bednárová L, Maloň P, Stokrová J. 2011. Lucifensin, a novel insect defensin of medicinal maggots: synthesis and structural study. *Chembiochem* 12: 1352–1361.

Charlet M, Chernysh S, Philippe H, Hetru C, Hoffmann JA, Bulet P. 1996. Innate immunity. Isolation of several cysteine-rich antimicrobial peptides from the blood of a mollusc, *Mytilus edulis*. *J Biol Chem.* 271:21808–21813.

Cociancich S, Goyffon M, Bontems F, Bulet P, Bouet F, Menez A, Hoffmann J. 1993. Purification and characterization of a scorpion defensin, a 4kDa antibacterial peptide presenting structural similarities with insect defensins and scorpion toxins. *Biochem Biophys Res Commun.* 194:17–22.

Coetzee WA, Amarillo Y, Chiu J, Chow A, Lau D, McCormack T, Moreno H, Nadal MS, Ozaita A, Pountney D, et al. 1999. Molecular diversity of K^+ channels. *Ann N Y Acad Sci.* 868:233–285.

Cohen L, Moran Y, Sharon A, Segal D, Gordon D, Gurevitz M. 2009. Drosomycin, an innate immunity peptide of *Drosophila melanogaster*, interacts with the fly voltage-gated sodium channel. *J Biol Chem.* 284:23558–23563.

Cornet B, Bonmatin JM, Hetru C, Hoffmann JA, Ptak M, Vovelle F. 1995. Refined three-dimensional solution structure of insect defensin A. *Structure* 3:435–448.

Corzo G, Papp F, Varga Z, Barraza O, Espino-Solis PG, Rodríguez de la Vega RC, Gaspar R, Panyi G, Possani LD. 2008. A selective blocker of $K_v1.2$ and $K_v1.3$ potassium channels from the venom of the scorpion *Centruroides suffusus suffusus*. *Biochem Pharmacol.* 76:1142–1154.

Crooks GE, Hon G, Chandonia JM, Brenner SE. 2004. WebLogo: a sequence logo generator. *Genome Res.* 14:1188–1190.

Delaglio F, Grzesiek S, Vuister GW, Zhu G, Pfeifer J, Bax A. 1995. NMRPipe: a multidimensional spectral processing system based on UNIX pipes. *J Biomol NMR.* 6:277–293.

Dimarcq JL, Bulet P, Hetru C, Hoffmann J. 1998. Cysteine-rich antimicrobial peptides in invertebrates. *Biopolymers* 47:465–477.

Duda TF Jr, Palumbi SR. 1999. Molecular genetics of ecological diversification: duplication and rapid evolution of toxin genes of the venomous gastropod *Conus*. *Proc Natl Acad Sci U S A.* 96:6820–6823.

Dutertre S, Lewis RJ. 2010. Use of venom peptides to probe ion channel structure and function. *J Biol Chem.* 285:13315–13320.

Ehret-Sabatier L, Loew D, Goyffon M, Fehlbaum P, Hoffmann JA, van Dorsselaer A, Bulet P. 1996. Characterization of novel cysteine-rich antimicrobial peptides from scorpion blood. *J Biol Chem.* 271: 29537–29544.

Fehlbaum P, Bulet P, Michaut L, Lagueux M, Broekaert WF, Hetru C, Hoffmann JA. 1994. Septic injury of *Drosophila* induces the synthesis of a potent antifungal peptide with sequence homology to plant antifungal peptides. *J Biol Chem.* 269:33159–33163.

Froy O, Gurevitz M. 1998. Membrane potential modulators: a thread of scarlet from plants to humans. *FASEB J.* 12:1793–1796.

Froy O, Gurevitz M. 2004. Arthropod defensins illuminate the divergence of scorpion neurotoxins. *J Pept Sci.* 10:714–718.

Froy O, Sagiv T, Poreh M, Urbach D, Zilberberg N, Gurevitz M. 1999. Dynamic diversification from a putative common ancestor of scorpion toxins affecting sodium, potassium, and chloride channels. *J Mol Evol.* 48:187–196.

Fry BG. 2005. From genome to "venome": molecular origin and evolution of the snake venom proteome inferred from phylogenetic analysis of toxin sequences and related body proteins. *Genome Res.* 15:403–420.

Fry BG, Roelants K, Champagne DE, Scheib H, Tyndall JD, King GF, Nevalainen TJ, Norman JA, Lewis RJ, Norton RS, et al. 2009. The toxicogenomic multiverse: convergent recruitment of proteins into animal venoms. *Annu Rev Genomics Hum Genet.* 10:483–511.

Gao B, Harvey PJ, Craik DJ, Ronjat M, De Waard M, Zhu S. 2013. Functional evolution of scorpion venom peptides with an inhibitor cystine knot fold. *Biosci Rep.* 33:3.

Gao B, Zhu S. 2010. Identification and characterization of the parasitic wasp *Nasonia* defensins: positive selection targeting the functional region? *Dev Comp Immunol.* 34:659–668.

Garcia ML, Gao YD, McManus OB, Kaczorowski GJ. 2001. Potassium channels: from scorpion venoms to high-resolution structure. *Toxicon* 39:739–748.

Garcia ML, Garcia-Calvo M, Hidalgo P, Lee A, MacKinnon R. 1994. Purification and characterization of three inhibitors of voltage-dependent K^+ channels from *Leiurus quinquestriatus var. hebraeus* venom. *Biochemistry* 33:6834–6839.

Goddard TD, Kneller DG. 2004. SPARKY 3. San Francisco (CA): University of California, San Francisco.

Goldin AL. 2002. Evolution of voltage-gated Na^+ channels. *J Exp Biol.* 205:575–584.

Hall BG, Malik HS. 1998. Determining the evolutionary potential of a gene. *Mol Biol Evol.* 15:1055–1061.

Heinig M, Frishman D. 2004. STRIDE: a web server for secondary structure assignment from known atomic coordinates of proteins. *Nucleic Acids Res.* 32:W500–W502.

Hidalgo P, MacKinnon R. 1995. Revealing the architecture of a K^+ channel pore through mutant cycles with a peptide inhibitor. *Science* 268:307–310.

Huys I, Dyason K, Waelkens E, Verdonck F, van Zyl J, du Plessis J, Müller GJ, van der Walt J, Clynen E, Schoofs L, et al. 2002. Purification, characterization and biosynthesis of parabutoxin 3, a component of *Parabuthus transvaalicus* venom. *Eur J Biochem.* 269:1854–1865.

Jeener J, Meier BH, Bachman P, Ernst RR. 1979. Investigation of exchange processes by two-dimensional NMR spectroscopy. *J Chem Phys.* 71: 4546–4533.

Jouirou B, Mosbah A, Visan V, Grissmer S, M'Barek S, Fajloun Z, Van Rietschoten J, Devaux C, Rochat H, Lippens G, et al. 2004. Cobatoxin 1 from *Centruroides noxius* scorpion venom: chemical synthesis, three-dimensional structure in solution, pharmacology and docking on K^+ channels. *Biochem J.* 377:37–49.

Kelly SM, Price NC. 2000. The use of circular dichroism in the investigation of protein structure and function. *Curr Protein Pept Sci.* 1: 349–384.

Kobayashi Y, Takashima H, Tamaoki H, Kyogoku Y, Lambert P, Kuroda H, Chino N, Watanabe TX, Kimura T, Sakakibara S, et al. 1991. The cystine-stabilized alpha-helix: a common structural motif of ion-channel blocking neurotoxic peptides. *Biopolymers* 31:1213–1220.

Koradi R, Billeter M, Wuthrich K. 1996. MOLMOL: a program for display and analysis of macromolecular structures. *J Mol Graph.* 14:51–55.

Landon C, Barbault F, Legrain M, Guenneugues M, Vovelle F. 2008. Rational design of peptides active against the gram positive bacteria *Staphylococcus aureus*. *Proteins* 72:229–239.

Lange A, Giller K, Hornig S, Martin-Eauclaire MF, Pongs O, Becker S, Baldus M. 2006. Toxin-induced conformational changes in a potassium channel revealed by solid-state NMR. *Nature* 440:959–962.

Laskowski RA, Rullmannn JA, MacArthur MW, Kaptein R, Thornton JM. 1996. AQUA and PROCHECK-NMR: programs for checking the quality of protein structures solved by NMR. *J Biomol NMR.* 8: 477–486.

Liman ER, Tytgat J, Hess P. 1992. Subunit stoichiometry of a mammalian K^+ channel determined by construction of multimeric cDNAs. *Neuron* 9:861–871.

López-Méndez B, Güntert P. 2006. Automated protein structure determination from NMR spectra. *J Am Chem Soc.* 128:13112–13122.

MacKinnon R, Cohen SL, Kuo A, Lee A, Chait BT. 1998. Structural conservation in prokaryotic and eukaryotic potassium channels. *Science* 280:106–109.

Mygind PH, Fischer RL, Schnorr KM, Hansen MT, Sönksen CP, Ludvigsen S, Raventós D, Buskov S, Christensen B, De Maria L, et al. 2005. Plectasin is a peptide antibiotic with therapeutic potential from a saprophytic fungus. *Nature* 437:975–980.

Park HS, Nam SH, Lee JK, Yoon CN, Mannervik B, Benkovic SJ, Kim HS. 2006. Design and evolution of new catalytic activity with an existing protein scaffold. *Science* 311:535–538.

Pascarella S, Argos P. 1992. Analysis of insertions/deletions in protein structures. *J Mol Biol.* 224:461–471.

Possani LD, Selisko B, Gurrola GB. 1999. Structure and function of scorpion toxins affecting K^+-channels. *Perspect Drug Discov.* 15(16):15–40.

Ranganathan R, Lewis JH, MacKinnon R. 1996. Spatial localization of the K^+ channel selectivity filter by mutant cycle-based structure analysis. *Neuron* 16:131–139.

Rendón-Anaya M, Delaye L, Possani LD, Herrera-Estrella A. 2012. Global transcriptome analysis of the scorpion *Centruroides noxius*: new toxin families and evolutionary insights from an ancestral scorpion species. *PLoS One* 7:e43331.

Rodríguez de la Vega RC, García BI, D'Ambrosio C, Diego-García E, Scaloni A, Possani LD. 2004. Antimicrobial peptide induction in the haemolymph of the Mexican scorpion *Centruroides limpidus limpidus* in response to septic injury. *Cell Mol Life Sci.* 61:1507–1519.

Rodriguez de la Vega RC, Possani LD. 2004. Current views on scorpion toxins specific for K^+-channels. *Toxicon* 43:865–875.

Saucedo AL, Flores-Solis D, Rodríguez de la Vega RC, Ramírez-Cordero B, Hernández-López R, Cano-Sánchez P, Noriega Navarro R, García-Valdés J, Coronas-Valderrama F, de Roodt A, et al. 2012. New tricks of an old pattern: structural versatility of scorpion toxins with common cysteine spacing. *J Biol Chem.* 287:12321–12330.

Selisko B, Garcia C, Becerril B, Gómez-Lagunas F, Garay C, Possani LD. 1998. Cobatoxins 1 and 2 from *Centruroides noxius* Hoffmann constitute a subfamily of potassium-channel-blocking scorpion toxins. *Eur J Biochem.* 254:468–479.

Srinivasan KN, Sivaraja V, Huys I, Sasaki T, Cheng B, Kumar TK, Sato K, Tytgat J, Yu C, San BC, et al. 2002. κ-Hefutoxin1, a novel toxin from the scorpion *Heterometrus fulvipes* with unique structure and function. Importance of the functional diad in potassium channel selectivity. *J Biol Chem.* 277:30040–30047.

Takeuchi K, Takahashi H, Sugai M, Iwai H, Kohno T, Sekimizu K, Natori S, Shimada I. 2004. Channel-forming membrane permeabilization by an antibacterial protein, sapecin. *J Biol Chem.* 279:4981–4987.

Tamura K, Dudley J, Nei M, Kumar S. 2007. MEGA4: Molecular Evolutionary Genetics Analysis (MEGA) software version 4.0. *Mol Biol Evol.* 24:1596–1599.

Tamura K, Peterson D, Peterson N, Stecher G, Nei M, Kumar S. 2011. MEGA5: molecular evolutionary genetics analysis using maximum likelihood, evolutionary distance, and maximum parsimony methods. *Mol Biol Evol.* 28:2731–2739.

Tian D, Wang Q, Zhang P, Araki H, Yang S, Kreitman M, Nagylaki T, Hudson R, Bergelson J, Chen JQ. 2008. Single-nucleotide mutation rate increases close to insertions/deletions in eukaryotes. *Nature* 455: 105–108.

Tordai H, Patthy L. 2004. Insertion of spliceosomal introns in protosplice sites: the case of secretory signal peptides. *FEBS Lett.* 575: 109–111.

Torres AM, Kuchel PW. 2004. The β-defensin-fold family of polypeptides. *Toxicon* 44:581–588.

Trautwein MD, Wiegmann BM, Beutel R, Kjer KM, Yeates DK. 2012. Advances in insect phylogeny at the dawn of the postgenomic era. *Annu Rev Entomol.* 57:449–468.

Tytgat J, Chandy KG, Garcia ML, Gutman GA, Martin-Eauclaire MF, van der Walt JJ, Possani LD. 1999. A unified nomenclature for short-chain peptides isolated from scorpion venoms: α-KTx molecular subfamilies. *Trends Pharmacol Sci.* 20:444–447.

Vibranovski MD, Sakabe NJ, de Souza SJ. 2006. A possible role of exon-shuffling in the evolution of signal peptides of human proteins. *FEBS Lett.* 580:1621–1624.

Xu W, Faisal M. 2010. Defensin of the zebra mussel (*Dreissena polymorpha*): molecular structure, *in vitro* expression, antimicrobial activity, and potential functions. *Mol Immunol.* 47:2138–2147.

Yount NY, Kupferwasser D, Spisni A, Dutz SM, Ramjan ZH, Sharma S, Waring AJ, Yeaman MR. 2009. Selective reciprocity in antimicrobial activity versus cytotoxicity of hBD-2 and crotamine. *Proc Natl Acad Sci U S A.* 106:14972–14977.

Yu JK, Wang MC, Shin-I T, Kohara Y, Holland LZ, Satoh N, Satou Y. 2008. A cDNA resource for the cephalochordate amphioxus *Branchiostoma floridae*. *Dev Genes Evol.* 218:723–727.

Zhu S. 2008. Discovery of six families of defensin-like peptides in fungi provides insights into origin and evolution of the CSαβ-type defensins. *Mol Immunol.* 45:828–838.

Zhu S, Darbon H, Dyason K, Verdonck F, Tytgat J. 2003. Evolutionary origin of inhibitor cystine knot peptides. *FASEB J.* 17:1765–1767.

Zhu S, Gao B. 2014. Nematode-derived drosomycin-type antifungal peptides provide evidence for plant-to-ecdysozoan horizontal transfer of a disease resistance gene. *Nat Commun.* 5:3154.

Zhu S, Gao B, Deng M, Yuan Y, Luo L, Peigneur S, Xiao Y, Liang S, Tytgat J. 2010. Drosotoxin, a selective inhibitor of tetrodotoxin-resistant sodium channels. *Biochem Pharmacol.* 80:1296–1302.

Zhu S, Gao B, Harvey P, Craik D. 2012. Dermatophytic defensin with antiinfective potential. *Proc Natl Acad Sci U S A.* 109:8495–8500.

Zhu S, Gao B, Tytgat J. 2005. Phylogenetic distribution, functional epitopes and evolution of the CSαβ superfamily. *Cell Mol Life Sci.* 62: 2257–2269.

Zhu S, Peigneur S, Gao B, Luo L, Jin D, Zhao Y, Tytgat J. 2011. Molecular diversity and functional evolution of scorpion potassium channel toxins. *Mol Cell Proteomics.* 10:M110.002832.